Available online www.jocpr.com

Journal of Chemical and Pharmaceutical Research, 2015, 7(3):2333-2346

Research Article

ISSN : 0975-7384
CODEN(USA) : JCPRC5

Effect of operating conditions on the performance of primary steam reformer in Basra fertilizer plant

Rand A. Abid and Ala'a A. Jassim

Chemical Eng. Department, College of Eng., Basra University, Basra, Iraq

---

ABSTRACT

The primary steam reformer (PSR) is the heart of Ammonia unite in Basra Fertilizer plant. It consists of catalyst tubes that located at the center of side-sired furnace. Steam reforming process of natural gas based on endothermic reactions is carried out in fixed bed reactors produce synthesis gas (CO and H_2). Three important limitations that affect the performance of PSR; thermodynamic equilibrium of reforming reactions, heat and mass transfer resistance and carbon formation. Two models are used in this study to simulate the PSR; radiative model for side-fired furnace and first order heterogeneous model or fixed bed reactor taking in account the above limitations. The simulation results is compared with operating data that carried on Basra fertilizer plant and they match well. The simulation program is used to discuss the effect of more important operating conditions; temperature, pressure and steam to methane ratio (SCR) of the feed, on composition of synthesis gas, reactor wall temperature, pressure drop and heat duty.

Keywords: Steam reforming, Ammonia production, Hydrogen production, Synthesis gas production

---

INTRODUCTION

Ammonia is one of the more important basic chemicals of the world, ranking with materials such as sulphoric acid and sodium carbonate. However it is a major end product as well as an important intermediate the production of more complex chemicals about 85% of ammonia consumption is used for the manufacture of fertilizer nitrogen. Converting of natural gas to synthesis gas by steam reforming is the first step to produce ammonia as shown in figure (1) [1].

Hydrocarbon, predominately methane in the economic climate and steam react in the presence of a catalyst material to form a mixture of hydrogen and carbon oxides, which are major chemical building blocks. The reforming reaction are highly endothermic, meaning that large quantities of heat must be added for the reaction to proceed. In Basra Fertilizer plant, reforming of natural gas is carried out with two stages; primary steam reforming where heat required for reactions is supplied from side fired furnace and secondary steam reformer which depends on partial oxidation of non converting methane to provide heat. Primary steam reformer consists of two parts radiation section and convection section. The radiation section is a furnace where combustion of natural gas is carried out to provide a required heat for steam reforming reaction. To increase the capacity of reformer, the radiation section consists of two parallel rectangular cells/chambers. Catalytic tubes are positioned at the center of each cell. To ensure the advantages provided by the side-fired configuration, small premix burners as shown in figure (2), lines up along the walls of the straight wall furnace, as such burners provide short flame length and ease for temperature control.

The commercial application of catalytic steam reformer was pioneered by BASF in 1926. This led to further development of reforming process using tubular reactor furnaces by 1930. Singh and Saraf, in 1979 [2], assumed that pore diffusion resistance for reformation reactions is very high. Singh and Saraf developed the following first-order kinetics expression which evaluated by Haldor topsoe for methane steam reforming and water gas shift

reaction. In 1989, Xu and Froment [3] have investigated methane steam reforming over $Ni/MgAl_2O_4$ catalyst in a tubular reactor. In their testing, H_2 was included in the feed to protect the Ni catalyst from re-oxidation by steam. By comparing the experimental data with the equilibrium constants, three reactions were identified as the major reactions in the reforming process. The authors proposed Langmuir–Hinshelwood (LH) type rate expressions for these reactions. In this study, kinetic that described by Xu and Froment to simulate the industrial steam reformer.

Industrial SMR is a mature technology. As a result, there exist many models in the academic and commercial literature that simulate steam-methane reformers. These models differ in their intended and in simplifying assumptions they use to describe reformer behavior. The complete models which can simulate the both of furnace-side and process side. Furnace-side models can be classified by the approaches used to describe the radiative heat transfer and furnace flow pattern. Process-side models can be classified by describing the fixed bed reactor in one or two dimension, mass and heat transfer limitation (homogenous or heterogeneous), kinetics reaction and pressure drop.

Singh and Saraf (1979) [2] used a version of the well-stirred model to generate tube-wall temperature profiles for an industrial SMR. In the Singh and Saraf version of the Hottel zone method, there are three zone types: burner surface, tube surface and furnace gas. It is assumed that the refractory is a no-flux zone (it reflects all incident radiation).Only two total-exchange areas are needed: the total-exchange area between the gas and an axial-tube zone, and between the burner surface and an axial-tube zone. The model that developed by Singh and Saraf was used by Soliman et al. (1988) [4] to simulate a side-fired reformer. Soliman et al. showed that reducing catalyst activity from 1.0 to 0.02 results in decreasing the methane conversion by 24% and the catalyst tube temperature increases by (5-6)%, while the furnace temperature increase by (10-11)%. In 2000, Rajesh et al. [5] develops a side-fired steam reformer model employing the kinetics of Xu and Froment, a non-iterative form of the furnace model of Singh and Saraf the calculation approach of Elnashaie et al. [6] for effective diffusivities. The authors report "a very good match is observed between the results obtained from our simulation and published industrial data". A two-step method to simulate the natural gas steam reforming for hydrogen production was performed by Olivieri and Veglio in 2008 [7]. The first step is to calculate reforming tube length and fuel distribution with equilibrium approach associated with heat transfer. The second step is to calculate and validate reforming performance with kinetic model. In 2011, a mathematical model was developed by Ajbar et al. [8] for a reformer used in the Midrex direct reduction plant. A steady state, one-dimensional model with negligible axial dispersion was adopted for the catalyst tubes. The furnace was, on the other hand, modeled with bottom firing configuration using two- flux Roesler method Ajbar et al. Proposed that a decrease in the inlet temperature causes evidently a decrease in methane conversion because of the endothermic reactions.

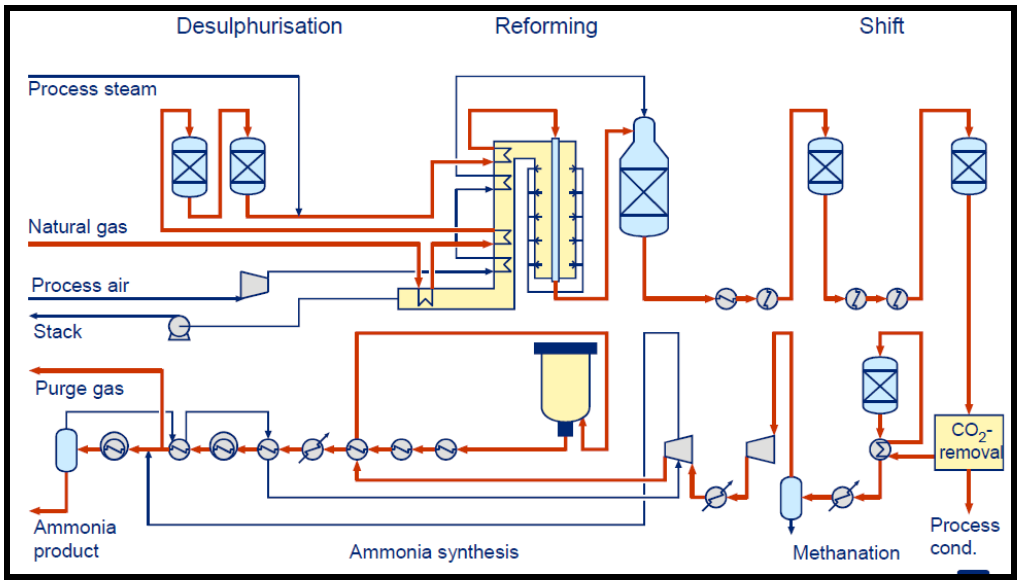

Figure (1) Process Scheme for Production of Ammonia Profertil of Haldor Topsoe [1]

2-Experimental work

2-1 Reactor side modeling:

2-1-1 Reaction Scheme and Kinetics:

In this study, the kinetic rate expression considered was developed by Xu and Forment [3], based on Langmuir-Hinshelwood (Hougen-Watson) approach, and using (Haldor Topsoe Ni/Al_2O_4 spinal). The mechanism model

consists of 13 steps, three of them are rate controlling; steam reforming reaction (SR), water gas shift (WGS) and reverse methanation reaction (RM) as shown below:

$CH_4 + H_2O \longleftrightarrow CO + 3H_2$ **(SR)** ΔH^0_{298}= 206 (kJ/mol) ....(1)

$CO + H_2O \longleftrightarrow CO_2 + H_2$ **(WGS)** ΔH^0_{298}= -41 (kJ/mol) ....(2)

$CH_4 + 2H_2O \longleftrightarrow CO_2 + 4H_2$ **(RM)** ΔH^0_{298}= 165(kJ/mol) ....(3)

A methane equivalent to the feed is calculated at the reactor entry; this is based on the assumption that higher hydrocarbons are very rapidly converted to methane by the following methanation reaction[2]:

$$C_nH_{2n+2}+\left(\frac{n-1}{2}\right)H_2O \rightarrow \left(\frac{3n+1}{4}\right)CH_4+\left(\frac{n-1}{4}\right)CO_2 \quad ....(4)$$

With the corresponding intrinsic rate equations of the first three reactions respectively [3]:

$$R_1 = \frac{k_1}{P_{H_2}^{2.5}.DEN^2}\left[P_{CH_4} * P_{H_2O} - \left(\frac{P_{H_2}^3 * P_{CO}}{K_{e,1}}\right)\right] \quad ....(5)$$

$$R_2 = \frac{k_2}{P_{H_2}.DEN^2}\left[P_{CO} * P_{H_2O} - \left(\frac{P_{H_2} * P_{CO2}}{K_{e,2}}\right)\right] \quad ....(6)$$

$$R_3 = \frac{k_3}{P_{H_2}^{3.5}.DEN^2}\left[P_{CH_4} * P_{H_2O}^2 - \left(\frac{P_{H_2}^4 * P_{CO2}}{K_{e,3}}\right)\right] \quad ....(7)$$

$$DEN = 1 + K_{ad,CO} * P_{CO} + K_{ad,H_2} * P_{H_2} + K_{ad,CH_4} * P_{CH_4} + \frac{K_{ad,H_2O} * P_{H_2O}}{P_{H_2}} \quad ....(8)$$

The equilibrium and rate constants can be evaluated by using the equations in reference [9].

2-1-2 Mass, heat and momentum balance:

The one-dimensional heterogeneous model is used here to study the component and temperature distribution along the catalyst tube. It is assumed that no carbon formation. From material and energy balances which is carried out over the cross section of tubular catalyst bed as shown in figure (2).

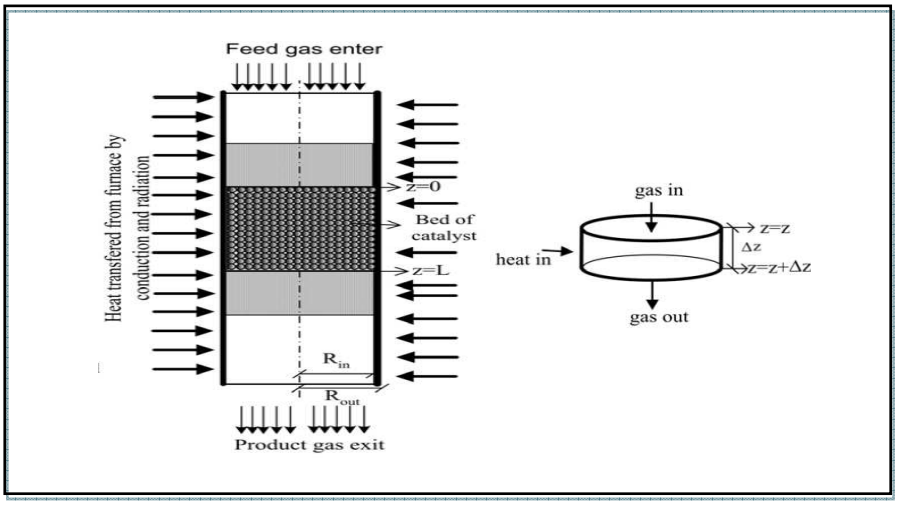

Figure (2) Schematic diagram of reactor configuration and control volume for model building

The continuity equations for each component in gas mixture can written in the following set of equation [10]:

$$\frac{dF_{CH_4}}{dZ} = -\rho c.(1-\varepsilon_B)A.(\eta_1.R_1+\eta_3.R_3) \quad ....(9)$$

$$\frac{dF_{H_2O}}{dZ} = -\rho c.(1-\varepsilon_B)A.(\eta_1.R_1+\eta_2.R_2+2\eta_3.R_3) \quad ....(10)$$

$$\frac{dF_{H_2}}{dZ} = \rho c.(1-\varepsilon_B)A.(3\eta_1.R_1+\eta_2.R_2+4\eta_3.R_3) \quad ....(11)$$

$$\frac{dF_{CO}}{dZ} = \rho c.(1-\varepsilon_B)A.(\eta_1.R_1-\eta_2.R_2) \quad ....(12)$$

$$\frac{dF_{CO_2}}{dZ} = \rho c.(1-\varepsilon_B)A.(\eta_2.R_2+\eta_3.R_3) \quad ....(13)$$

The change in the temperature throughout the reactor length has been given by various authors[10]:

$$\frac{dT_g}{dZ} = \frac{\sum_{k=1}^{3}(-\Delta H_{r,k})\rho c.(1-\varepsilon_B)A.R_k + \pi.d_{t,i}q}{\sum F_i.C_{pi}} \quad ....(14)$$

For the flow through a ring packing often used in industrial packed columns, the Ergun equation is considered as a good semi-empirical correlation for predicting the pressure drop as follows [10]:

$$\frac{dP}{dZ} = -\left[\frac{150(1-\varepsilon_B)^2.\mu g.u_g}{\varepsilon_B^3.d_p^2} + \frac{1.75((1-\varepsilon_B).\rho_g.u_g^2}{\varepsilon_B^3.d_p}\right] \quad ....(15)$$

2-1-3 Effectiveness factor estimation:

The intra particle diffusion resistance is mainly influenced by the characteristics of catalyst pellet (shape and size). Therefore, the effectiveness factor should be considered in order to apply the kinetic equation to the industrial reformer design. For the spherical catalyst pellet, the effectiveness factor can be evaluated using the following equation. [10,11,12]:

$$\eta_k = \frac{1}{\varphi}\left[\frac{1}{\tanh(3\varphi)} - \frac{1}{3\varphi}\right] \quad ....(16)$$

$$\varphi_k = \frac{d_p}{6}\sqrt{\frac{k_{v,k}\rho_{cat}(1+K_{e,k})}{K_{e,k}.D_k}} \quad ....(17)$$

$$k_{v,1} = k_1 * 0.08314 * T/P_{tot}^{1.5} \quad ....(18)$$

$$k_{v,2} = k_2 * 0.08314 * T \quad ....(19)$$

$$k_{v,3} = k_3 * 0.08314 * T/P_{tot}^{1.5} \quad ....(20)$$

The effective diffusivity becomes as the following equation [13]:

$$De_k = \frac{\varepsilon_p}{\tau}\left[\frac{D_{kn,i} * D_{i,mix}}{D_{kn,i} + D_{i,mix}}\right] \quad ....(21)$$

The selected catalyst particle is the industrial Haldor Topsoe R-67-7H (tablet shape with seven holes and convex ends). The complex geometry of the real particle is represented by means of an equivalent spherical model. The equivalent pellet diameter and other characteristics are listed in table (1).

2-2 Furnace-Side Modeling:

A typical side-fired steam reformer is shown in figure (3), with process gas flowing downwards through multiple tubes in a single row, all of which are contained within one or more compartments known as furnace cells. This design is based on the concept of uniform heat flux. achieved by positioning the catalyst tubes in the centre of the furnace cell with heat input provided by burners. Burners are located along the entire sidewall of the furnace and arranged in six rows. Flue gas exhausts at the top of the furnace and is directly connected with the convection section.

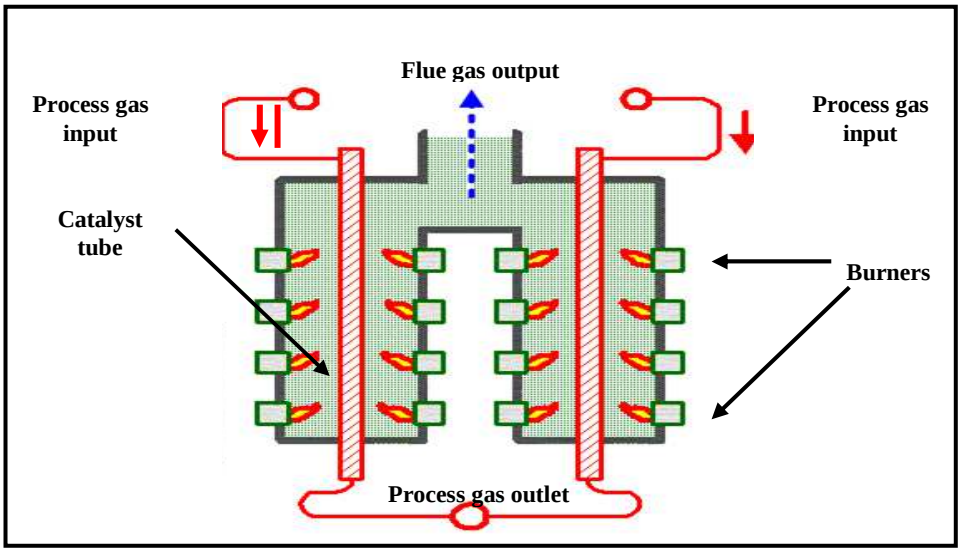

Figure (3) Schematic diagram of side fire Furnace

The heat balance on radiation section:[14],

$$Q_{in} = Q_R + Q_g + Q_L$$

$$Q_{in} = m_f \,.LHV + Q_{air} + Q_f$$

$$Q_R = Q_{rad} + Q_{conv}$$

$$Q_g = m_g \,.cp_g (T_{ex} - T_{ref})$$

The following simplifying assumptions are made to be able to describe the side fire furnace:

1. Radiation is the prevailing mode for transfer of heat by furnace gas and flames. Heat transferred by conduction and convection is negligible compared to the total amount of heat received by the reformer tubes.
2. The fuel is burnt completely and the combustion products (furnace gas) is gray gas[2].
3. There is no distinction between different elements of reformer tube surface due to geometrical disposition or proximity to burner [2].
4. Flames radiate at adiabatic flame and the radiation from furnace gas and tubes absorbed by flames are negligible [2].

Hence, the total heat flux from gas combustion gas and flame to tube surface is :[5]

$$q_{rad} = \frac{\sigma.(A_{t,o} + A_R).\varepsilon_g.\varepsilon_t}{(A_{t,o} + A_R).\varepsilon_g + A_{t,o}.(1-\varepsilon_g).\varepsilon_t}(T_g^4 - T_{t,o}^4) + \frac{\sigma.N_B.A_f.\varepsilon_f.(1-\varepsilon_g).\varepsilon_t T_f^4}{A_{t,o}} \quad \text{....(22)}$$

While, the overall heat flux across the tube wall to process gas is:

$$q = U_{in}(T_{t,o} - T) \quad \text{....(23)}$$

Where:

$$\frac{1}{U_{in}} = \frac{d_{ti}}{2\lambda_t} \ln \frac{d_{to}}{d_{ti}} + \frac{1}{h_i} \quad \text{...(24)}$$

$$h_{in} = 0.4 * \frac{kg}{Dp} \left[2.58 Re_p^{1/3} Pr^{1/3} + 0.094 Re_p^{0.8} Pr^{0.4} \right] \quad \text{....(25)}$$

The temperature of outer wall can be calculated by equating the fluxes due to radiative heat transfer from furnace, eq.(22), and conductive-convective heat transfer across tube wall , eq.(23).
Where;

$$q_R = d_{ti} q / d_{t,o} \quad \text{....(26)}$$

2-3 Numerical Solution Strategy :
The heat transfer equations describing the furnace can be decoupled from those describing the reaction in the reformer tubes by assuming initial values for wall and gas temperature. For furnace side, heat of combustion and flame temperature are calculated and radiation heat by using the assumed values of flue gas and wall temperature. Consecutive iteration is carried out between furnace and tube equations until two iteration match. Assuming of wall temperature value is repeated on each step along the catalyst tube to predict the wall temperature profile. On each step, the correct value of wall temperature is used to calculate the heat flux on the tube wall. For tube side the calculation starts from the top end of tube where the process gas is fed , Since the inlet conditions of process gas is known, the reaction rates, diffusivities and effectiveness factor can be estimated.

The differential equation that describe composition and temperature profile and pressure drop can be solved numerically using Euler method. The calculation is repeated on each step along catalyst tube until the exit point of process gas reach. The total heat flux is determined then compared with heat balance on furnace to predict the true value of flue gas temperature. Otherwise a new value of flue gas temperature is reassumed and the procedure of calculation along reactor length is repeated.

RESULTS AND DISCUSSION

The equivalent feed and the operation conditions of process gas stream is taken from data sheet of industrial primary reformer in Basra fertilizer plant at 100 % load which are tabulated in the table (2):

3-1 Model Validation:
In this study, a side-fired primary reformer is modeled mathematically. The actual industrial conditions of Basra Fertilizer plant of ammonia unit is used as input data to simulation program. The comparison between simulation results and actual plant information is presented in table (3). A Good agreement between measured and calculated values is an indication of good performance of the model.

Though the steam reforming reaction tends to reach equilibrium state, the actual product composition has a gap from its chemical equilibrium state at the outlet temperature.

3-2 Component distribution in the catalyst bed:
Mass balance of the five components of steam reforming process is carried out using one-dimensional heterogeneous modeling for fixed bed reactor. Figure (4) describes the steady state behavior of the molar fractions along the catalyst bed. As anticipated H_2 is formed at the expense of CH_4 and steam. As can be seen in this figure, the CO content is very low up to 5 meters, because the shift reaction goes to equilibrium easily as reported by Khomenko et al.[15]. However, the CO_2 fraction would not increase further over 11 meters, because the WGS reaction is exothermic, while the hydrogen content increases further because the methane steam reforming action is endothermic. It is also evident that CO is more than CO_2 at the reactor exit, which is the result of the WGS reaction being reversed at high temperature due to its exothermic nature.

3-3 Temperature distribution in the catalyst bed:
The temperature profile of process gas and tube wall along the catalyst bed are shown in figure (5). The two curves highlight a non- monotonic trend at low temperatures. A temperature decreasing is present close to the tube inlet due to the high endothermic nature of steam reforming reactions. When the distance from the tube inlet rises (more than

1 m), process gas temperature increases with a monotonic trend. This is achieved when the transferred energy is sufficient to supply total reaction enthalpy and sensible heat for temperature increasing. The same behavior is noticed for the profile curve of tube wall temperature. The maximum wall temperature is recorded at reformer exit because of constant heat flux of side fired furnace as reported by Rajesh [5] and Oliveri [7] comparing with top and bottom fired furnaces where the maximum wall temperature is recorded at the first or second third of bed height [16]. In any case, the highest wall temperature should not exceed the design reactor wall value to avoid the tube rupture [7].

Table (1) Design data of radiant section of (PSR)

Chamber Dimension	
Height (m)	11.4
Length (m)	27.255
Width (m)	1.84
Catalyst Tubes	
Number of tubes	2*100
Inner tube diameter (m)	0.118
Outer tube diameter (m)	0.152
Heated tube length (m)	11.4
Overall tube length including hairpin (m)	12.815
Catalyst volume, installed (m^3)	25.1
Tube material	24/24 Nb
Design tube wall temperature ^0C	895
Burners	
Number of burners	2*240
Type of burners	Self-aspirating wall burner
Burner diameter	11 cm
Normal heat release per burner, LHV	250,000 kcal/h
Maximum heat release per burner, LHV	315,000 kcal/h
Fuel type	Natural gas
Catalyst	
Catalyst type (Haldor Topsoe)	R-67-7H
Shape	cylinder with 7 holes
Size (O.D* H) mm	16*11
Hole diameter (mm)	3.4
Bulk density (kg/m^3)	970
Void volume	0.5
Average radius pore (A^o)	80
Tortuous	2.74

Table (2) Equivalent feed and operation condition of process gas stream in Primary reformer unite

Parameter	Value
Flowrate of natural gas fuel (kmol/h)	560.625
Excess air (%)	10
Temperature of fuel and air (^oC)	25
LHV of fuel (kJ/kmol)	9.41E+05
Natural gas process temperature (^oC)	505
Natural gas process pressure (bar)	34.3
Steam/CH_{4eq}	3.97
Molar flowrate of equivalent process feed (kmol/h)	
F_{CH4}	1227.94
F_{H2}	47.99
F_{CO}	0
F_{CO2}	90.592
$F_{(N2+Ar)}$	27.14
F_{H2O}	4874.84

3-4 The approach to equilibrium:

Figure (6) depicts the approach to equilibrium profile for three reactions in term of ratio of partial pressure of reactants and products to rate constant. In case of the two steam reforming reactions, It is only slowly increases to 72% of equilibrium at the exit of reactor because the rising process gas temperature shifts the equilibrium of these reactions further to the right. While the WGS reaction exceeds the equilibrium at the same position. Figure (7) also shows, the local difference between the actual process gas temperature and the temperature that would be reached if the process gas were at equilibrium. This difference is often used to characterize the operation of an industrial reformer. Its value is about 14°C at the reformer exit.

Table(3) Comparisons between plants data and model predictions at the primary reformer exit

Property	Output		Error percentage
	Plant	Predicted	
Flue gas temperature (°C)	1030	980	4.9
Flue gas flowrate (kmol/h)	8195.31	8195	0.004
Process gas temperature (°C)	784	781	0.38
Process gas pressure (bar)	32	32.03	0.1
Dry gas flowrate (kmol/h)	4219.82	4141.46	1.9
Steam/dry gas	0.86	0.89	3.5
Dry process gas composition (mol%)			
CH_4	10.2	11	7.84
CO_2	8.68	8.28	4.6
CO	12.38	12.56	1.45
H_2	68.1	67.51	0.87
(N_2+Ar)	0.64	0.66	3.125
ATE (°C)	-	13.85	
Maximum wall temp. (°C)	-	885.85	

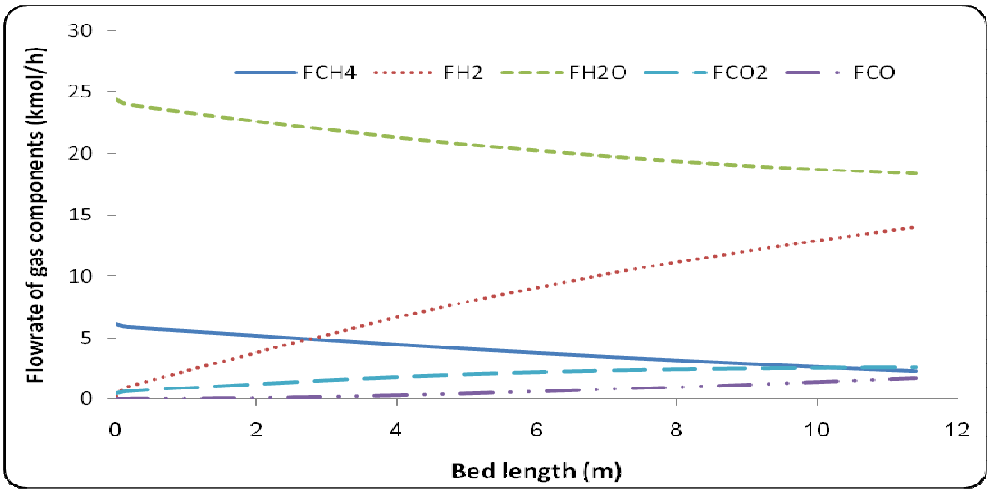

Figure (4) Component distribution along the reformer length relative to inlet operation conditions (P=34.3bar, T=505 °C &SCR=3.97)

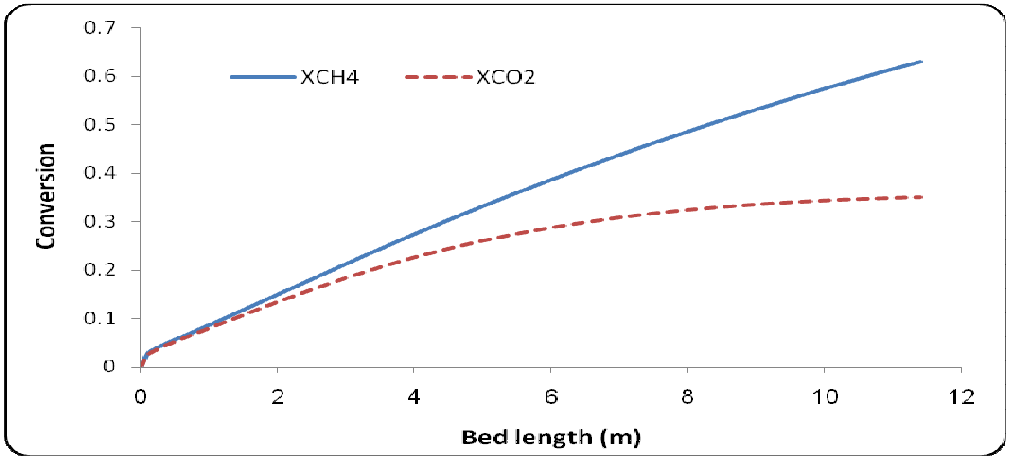

Figure (5) conversion profile of CH_4 and CO_2 along the reformer length relative to inlet operation conditions (P=34.3bar, T=505 °C & SCR=3.97)

3-5 Pressure drop Prediction:

Figure (8) shows that the pressure of process gas have reduces at the exit reformer from (34.3 to 32). The decline of pressure along the reactor has occurred as a result to the friction between particle of gases, particles of gases with catalyst pellet and with walls of reactor. Pressure drop is the key parameter in the steam reforming reactor. From one hand, low pressure drop is a desirable characteristic of a particular catalyst shape, because of a lower mechanical energy loss.

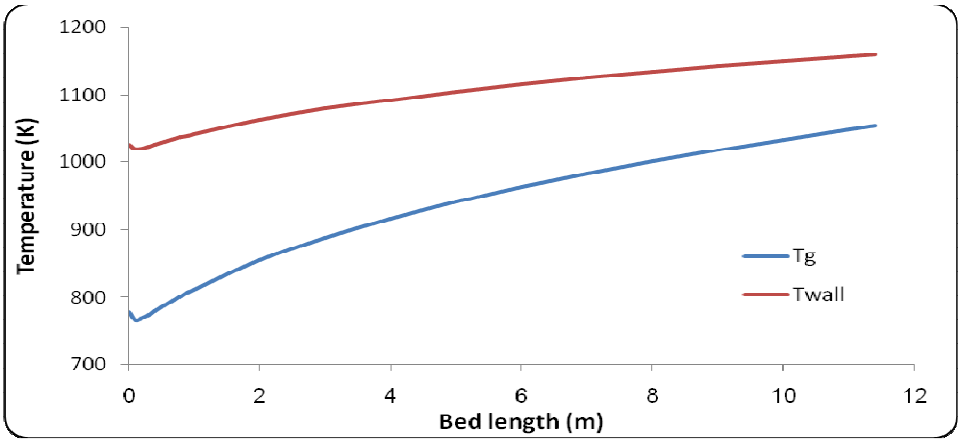

Figure (6) Temperature distribution along the reformer length relative to inlet operation conditions (P=34.3bar, T=505 ºC &SCR=3.97)

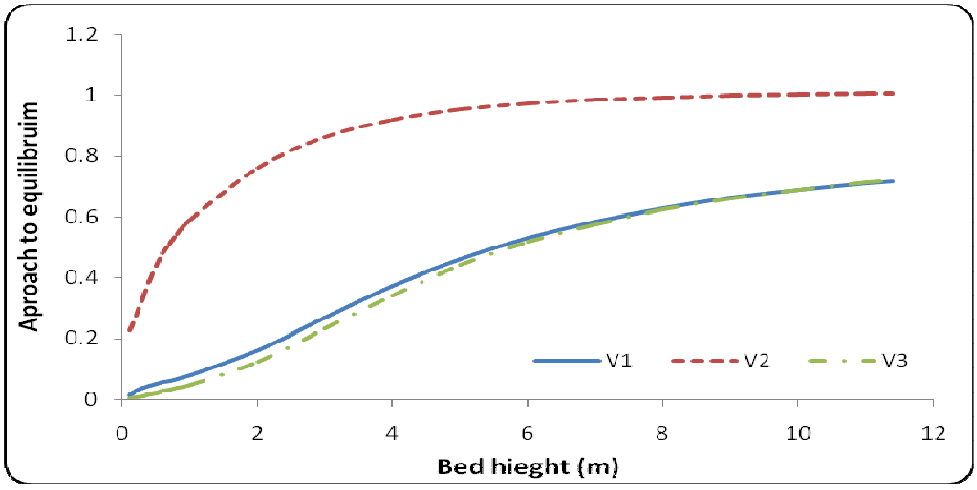

Figure (7) Approach to equilibrium in term equilibrium constant along the reformer length relative to inlet operation conditions (P=34.3bar, T=505 ºC &SCR=3.97)

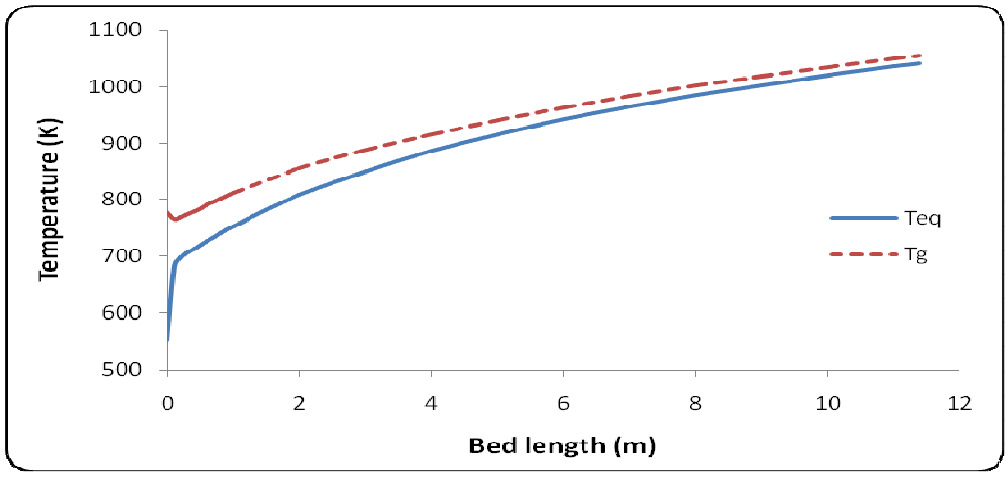

Figure (8) Approach to equilibrium in term equilibrium temperature along the reformer length relative to inlet operation conditions (P=34.3bar, T=505 ºC &SCR=3.97)

3-6 Heat flux profile:

The side fired furnace relies upon the tube being bounded on two sides by a refractory wall. In ammonia plant, 60 % of the heat received by the tubes from the radiating refractory wall is required to endothermic reactions and 40% to raise the temperature to the level of reformer exit. The value of heat flux depends on the difference of wall and process gas temperatures. Figure (9) illustrates the heat flux profile along axial direction of catalytic tube. The maximum heat flux is positioned at the reactor inlet where the amount of heat flux value gradually decreases as the

difference of two temperatures are reduced. Integrating the area under the curve and dividing by bed axial length gives the average heat duty for one tube in steam reformer, which is limited to be (79.57 kW/m^2).The value of absorbed heat is agreed with the typical range of heat duty that reported by Rostrup-Nielsen which is a (45-90) kW/m^2 [17].

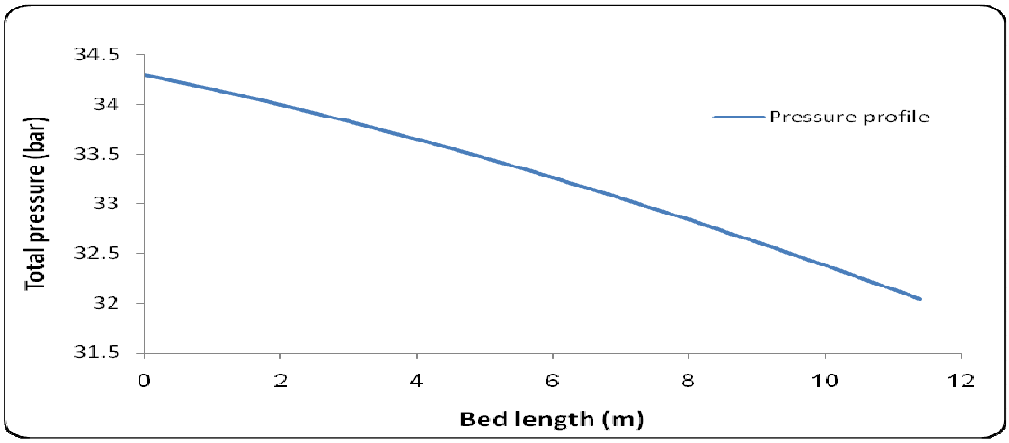

Figure (9) total pressure distribution along the reformer length relative to inlet operation conditions (P=34.3bar, T=505 ºC &SCR=3.97)

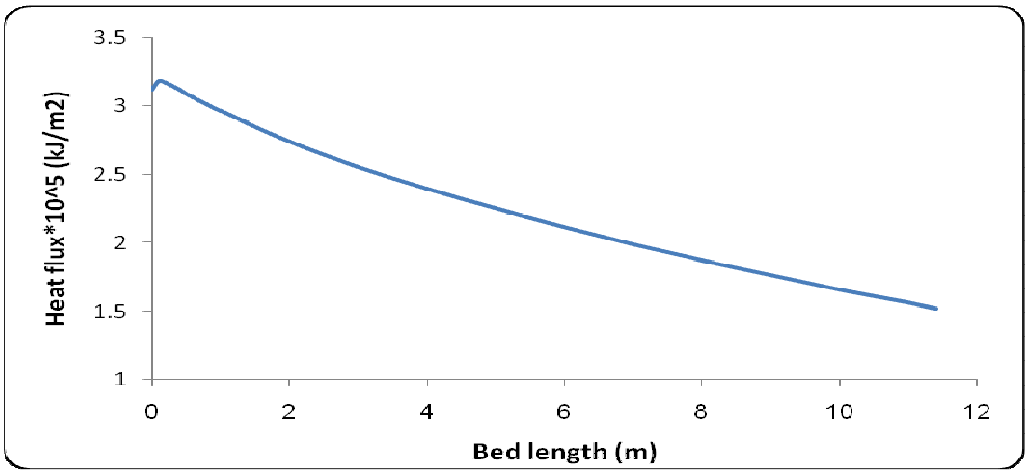

Figure (10) Heat flux profile along the reformer length relative to inlet operation conditions (P=34.3bar, T=505 ºC &SCR=3.97)

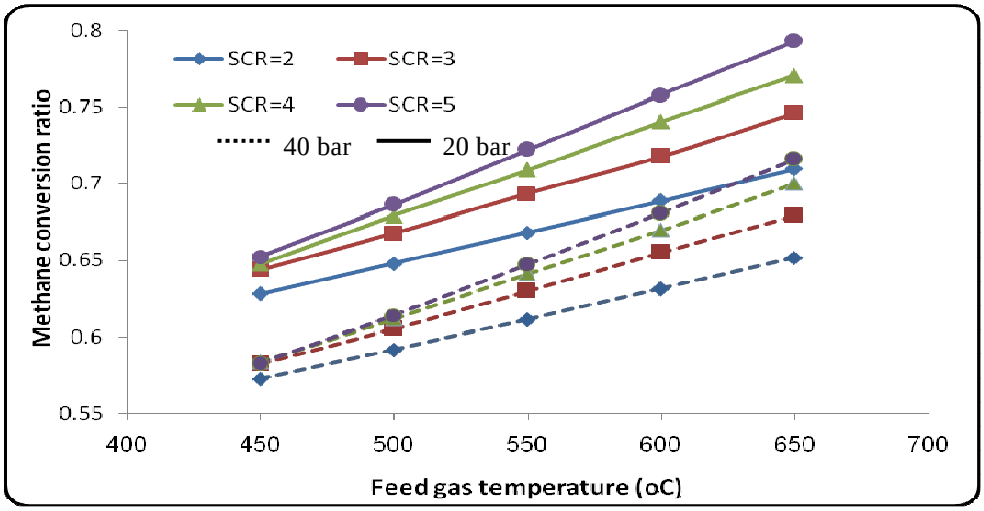

Figure (11) Methane conversion as a function to feed gas temperature, pressure and SCR

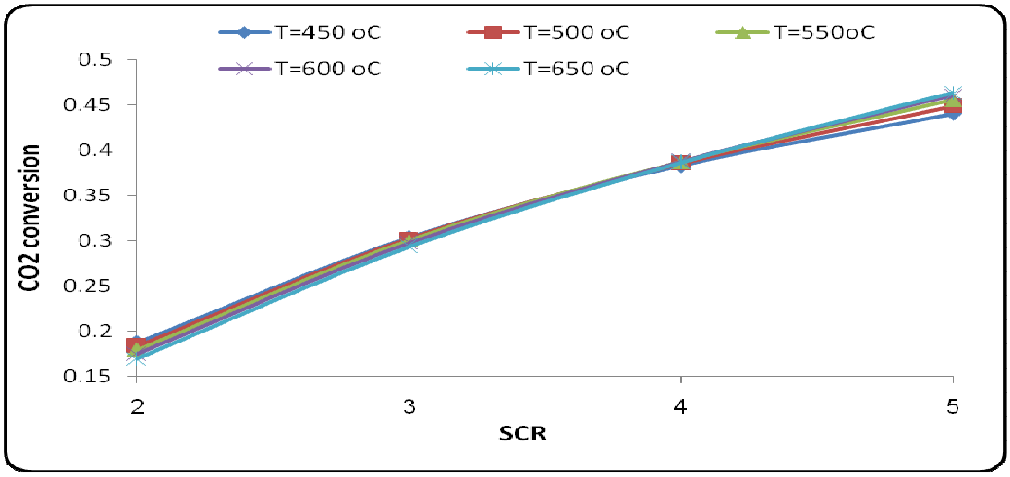

Figure (12) CO_2 conversion as a function to feed gas temperature and SCR at 20 bar

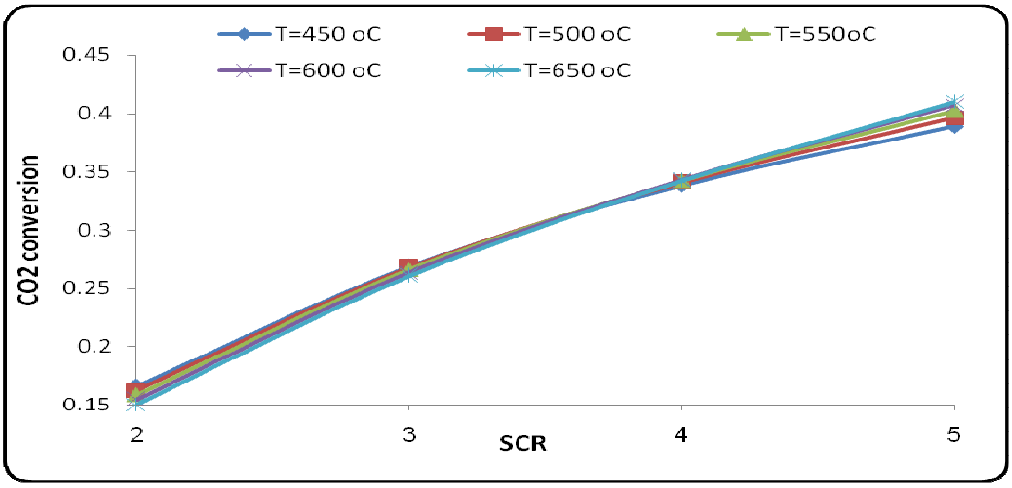

Figure (13) CO_2 conversion as a function to feed gas temperature and SCR at 40 bar

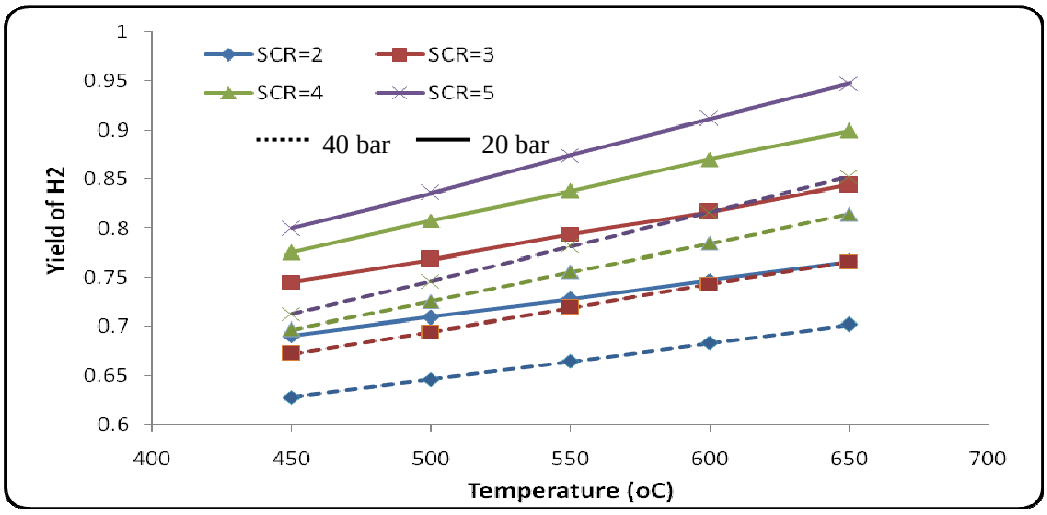

Figure (14) Effect of operating pressure ,temperature and SCR on hydrogen yield

3-7 Operation Conditions Effect:

The performance of primary reformer is affected by the operating parameters, such as feed gas pressure, temperature and steam to methane ratio (S/CH_4).. In this study the performance of conventional reformer is studied with altering the operating condition feed temperature (450 -650)^oC, feed pressure (20-40) bar and SCR (2-5). Kinetic model is necessary to evaluate the influence of the more important operation conditions not only on hydrogen and CO yield, also on pressure drop, heat duty and temperature of outer reactor wall .

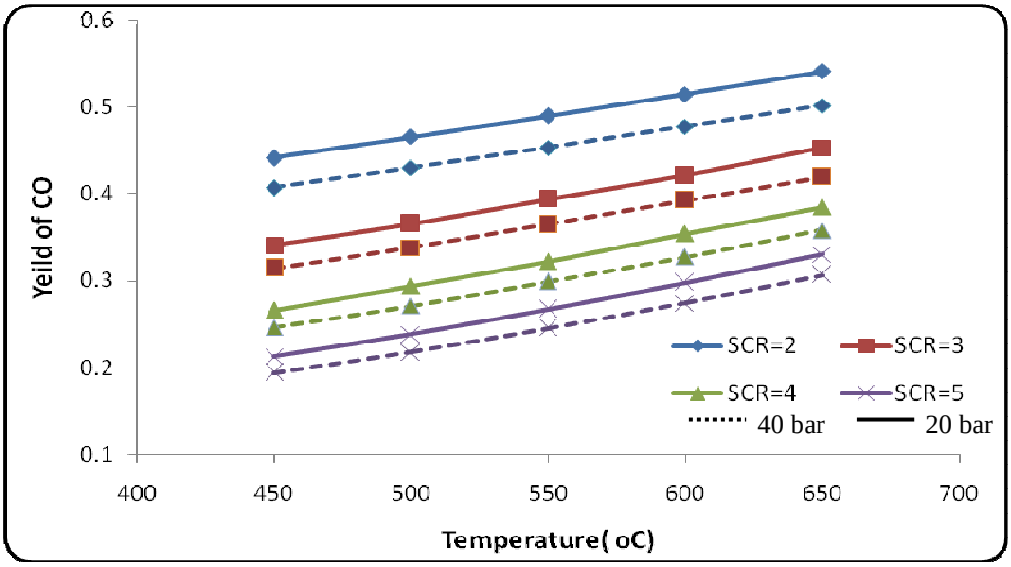

Figure (15) Effect of operating pressure, temperature and SCR on CO yield

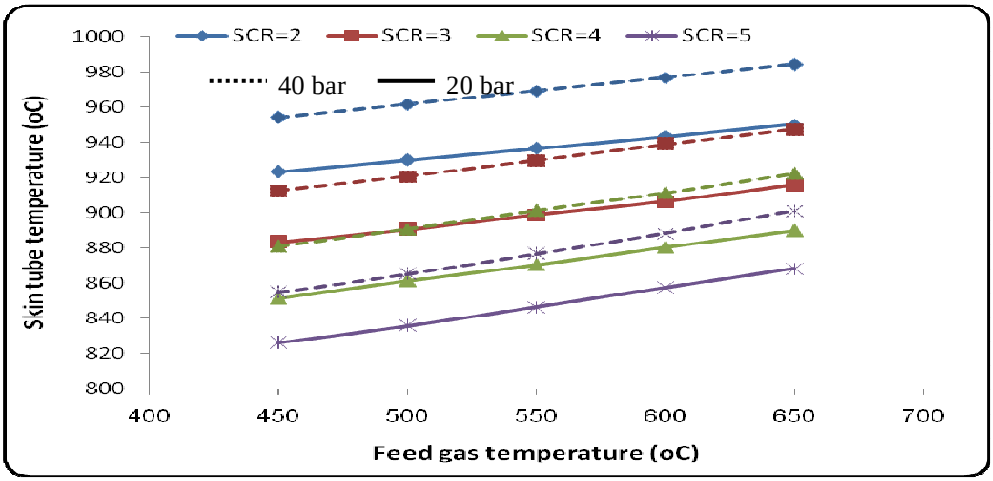

Figure (16) Skin tube temperature as a function to feed gas temperature, pressure and SCR

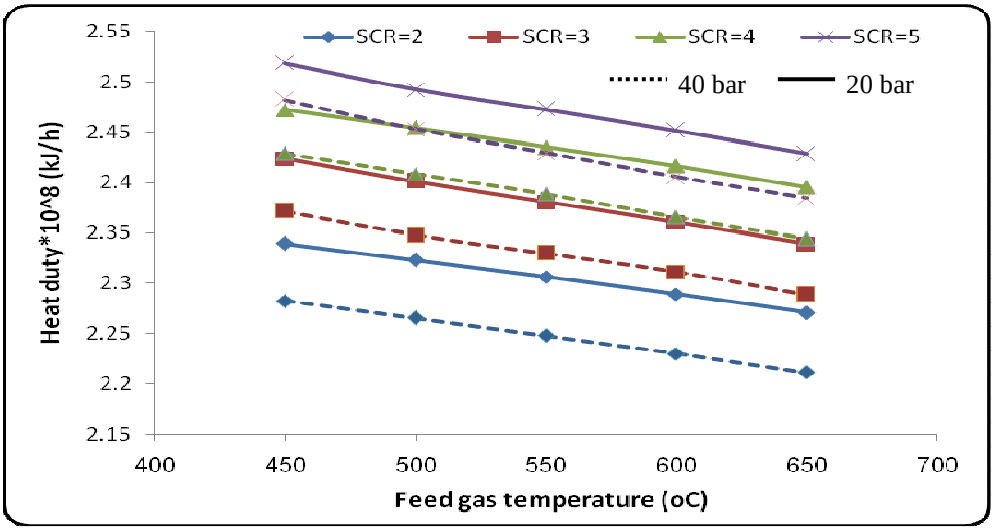

Figure (17) Average heat absorbed by reformer as a function to feed gas temperature, pressure and SCR

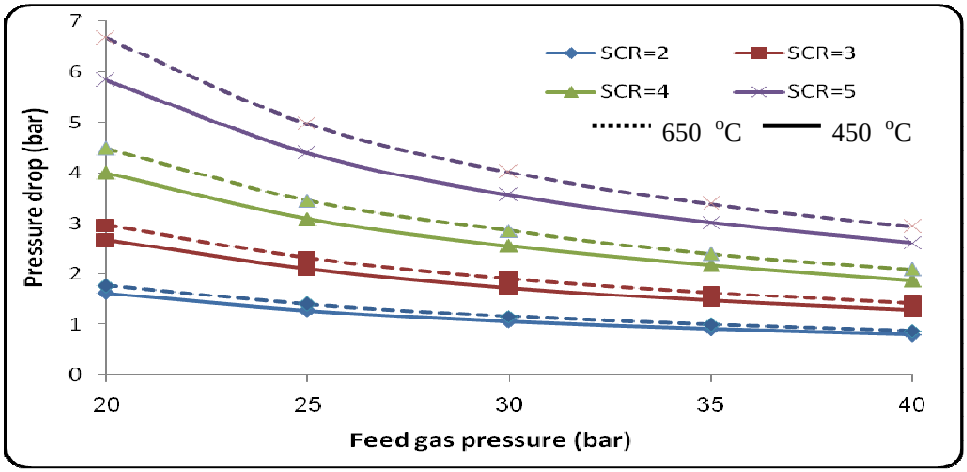

Figure (18) Pressure drop as a function to feed gas pressure, temperature and SCR

3-7-1 Conversion of CH_4 and CO_2:

The reaction temperature plays an important role in the reactor performance via thermodynamic and kinetics. Thermodynamically, at fixed pressure and (SCR), increasing of feed temperature results in shifting the endothermic reaction to right side. Le- Chatelier's principle states, increasing the pressure favors the side of the equilibrium with the least number of gaseous molecules. Therefore; the rate of steam reforming reactions decreases whereas there is no effect of pressure on WGS reaction. At equilibrium reactions, increasing the moles of one reactant shifts the reaction rate toward another side. The molar flowrate of steam in feed gas process is pointed here as steam to methane ratio (SCR). The SCR is an important parameter affecting hydrocarbon steam reforming. The relationship between methane conversion as a function to inlet gas temperature and steam to methane ratio at constant pressure is shown in figure (10). Increasing the feed process gas temperature has no effect on CO2 conversion at SCR (3-4). The effect of temperature rising has negative effect on CO2 conversion at SCR=2 while , the behavior of conversion reverses with temperature increasing at SCR=5. Pressure rising has slightly effect on CO2 conversion.

3-7-2 Yield of H_2 and CO:

It is shown from figure (11) that yield of hydrogen increases with increasing feed temperature and SCR dues to rising the conversion of two reforming reactions. It is obvious that response of yield with temperature increasing rises with increasing SCR. However the maximum yield of H2 is recorded at higher temperature and SCR. While rising of operation pressure has a negative effect H_2 yield. It can be concluded from figure that negative effect of operating pressure can be overcome by increasing feed temperature or SCR or both of them. Figure (12) shows that effect of pressure increasing has negative effect on CO yield than H2.

3-7-3 Temperature of gas process and skin tube:

In Side fired reformer, the maximum skin tube temperature is at the reformer exit. To ensure long operation life of tube, maximum temperature must not exceed the tube design temperature. In general increasing the feed process gas temperature from 500^{o}C to 650^{o}C, at constant pressure and SCR, results in rising the skin tube temperature. It is recommended to limit the maximum exit gas temperature to 900 ^{o}C to avoid the melting of the catalyst [18]. Figure (13) shows the effect of feed process gas temperature, pressure and SCR on the skin tube temperature. It is illustrates lower tube skin temperature is produced at lower temperature and pressure and higher SCR.

3-7-4 Heat Load:

The influence of three conditions on total heat absorbed from furnace is analyzed in figure (14). It is shown that using higher inlet process gas temperature can lessen the heat duty. However increasing of absorbed heat indicates to increasing of reforming reaction rate. Therefore increasing of operating pressure at low SCR leads to higher reduction in total heat absorbed. Rising of SCR can compensate the heat transfer decreasing with high pressure.

3-7-5 Pressure drop:

To study the influence of three important operation conditions change on pressure drop, figure (15) shows that maximum pressure drop appears at the lowest and the highest temperature and SCR. While minimum pressure drop is at the highest pressure, less temperature and SCR. This result is proportional with minimum and maximum yield of hydrogen as shown above in figure (11). Therefore it is important to balance between maximum yield and minimum pressure drop.

CONCLUSION

This paper is an attempt to modeling and simulation the Primary Steam Reformer taking in account all limitations: thermodynamic equilibrium, mass and heat transfer resistance. The simulation results gave a good agreement when compared with data of reformer exit operates at the same conditions. The Simulation program is used to describe the behavior of composition and temperature and pressure and heat flux profile throughout packed bed length. The effect of three important operation conditions on the Primary steam reformer performance is analyzed. The performance variables of industrial steam reformer are: yield of H2 and CO, tube skin temperature, pressure drop and heat duty. It is found that important to make balance among the values of operation conditions to reach to optimum performance.

Acknowledgements
The authors would like to acknowledge to the workers in steam reforming unite in Ammonia plant of Basra Fertilizer plant for their assistance.

REFERENCES

[1] Rostrup-J.R Nielsen. Steam reforming Catalysts, Haldor Topsoe, **1974**.
[2] Chandra P.P. Singh, Deoki N. Saraf, *Ind. Eng.Chem. process Des. Dev*., **1979**,18, (1-7).
[3] J. Xu, Gilbert F. Froment, *AlChE Journal*, **1989**,I.,35(1), (88-103).
[4] J.K.Rajesh,Santosh K.Gupta, G.P.Rangaiah, Ajay K.Ray, *Ind.Eng.Res.*, **2000**,39,(706-717)
[5] S.S.E.Elnashaie, A.M. Adris,M. A. Soliman, A. S. Al-Ubaid, *The Candian J. of Chemical Engineering*.**1992**, V(70), August, (786-793).
[6] A.Olivieri, F. Veglio, *Fuel Processing Technology*, **2008**,89,(622-632).
[7] A. Ajbar, K. Alhumaizi *J. Chem. Eng*.28(12),2242-2249,
[8] M. Soliman, Korean L. Chibane, B. Djellouli, *International J. of Chemical Eng. And Application*, **2011**, 2(3), (147-155).
[9] G. F. Forment, K. B. Bischoff, J. De Wilde, *Chemical Reactor Analysis and Design, 3rd Edition, John Wiley* & Sons, USA, **2009**, (493-513).
[10] K. Vakhshouri, M.M.Y. Hashemi, *World Academy of Science, Engineering and Technology*, **2007**,34,180-186.
[11] Yong H. Yu, M. H. Sonsa, *Korean J. Chem. Eng*., 2001,18(1), 127-132.
[12] Xu, Gilbert F. Froment, *AlChE Journal*, **1989**,II.,35(1), (88-103).
[13] Donald Q.Kern, *Process Heat Transfer*,*23rd Edition, International Student Edition, Singapore*, 1986, 699.
[14] Young Yu, *Chem. Eng. Technol*., **2002**, 25(3), 307-313.
[15] D. A. Latham, K. B. McAuley, B. A. Peppley, T. M. Raybold**,** *Fuel Processing Technology*, **2011**,92, 1574-1586.
[16] Rostrup-J.R Nielsen; Jens K. Norskov, *Avan. Cata.J*.,**2002**,47,(65-139).
[17] B.Maza, *World Academy of Science, Engineering and Technology*, **2001,** 71, 181-186.